Characterization of distribution parameters of fragment mass and number for conventional projectiles

Berko Zecevic*, Jasmin Terzic*, Alan Catovic*,
and Sabina Serdarevic-Kadic*

* University of Sarajevo, Mechanical Engineering faculty, Bosnia and Herzegovina

zecevic@mef.unsa.ba

Abstract:

Assessment of parameters of high explosive (HE) projectile fragmentation process (mass distribution and number of fragments) in most of the scientific papers is generally best described using Mott (depending on dimensionality and different scaling models) and Held equations. These methods can describe mass distribution of fragments excellent, but precise data about individual parameters from these equations are not available in public literature. During the previous eksperimental research of natural fragmentation for several types of HE projectiles, authors are studied the effects of several types of projectile body materials, two types of high explosive and projectile design and determined range of parameters using in Held laws. Obtained data can help designers with smaller experimental experience to make faster prediction of new projectile fragmentation parameters.

Keywords: Natural fragmentation; Mass distribution; Held methodology

1 Introduction

Natural fragmentation of projectiles or warheads results in the formation of a large number of fragments of different masses and geometries. Expansion of projectile body by detonation products of explosive charge causes a warhead to split into various sized fragments.

Fragment mass distribution depends on warhead geometry, diameter and length of explosive charge, thickness of projectile body, body material, its mechanical characteristics and thermal treatment, as well as explosive charge type.

Determination of warhead performances requires very complex measuring equipment and measuring process itself is expensive as well. Number, mass and shape of fragments are generally determined in Pit test. Spatial distribution of fragments can be determined using Arena test. In more complex Arena tests, fragments can be caught and their velocity could be determined, while in simpler Arena tests, only fragment spatial density is measured.

The authors used the results of a large number of tests, and applied statistical and numerical methods.

Capability to make warhead performance prediction in the earliest phases of ammunition or warheads preliminary design is crucial. Ability for warhead performances prediction depends on comprehensive data base of warheads natural fragmentation features, including data on fragment mass, number and shape, initial fragment velocities, warhead case and explosive material performances and spatial fragment distributions.

Using experimental test of natural fragmentation for several types of high explosive projectiles and available numerical and statistical techniques, authors tried to show basic natural fragmentation peremeters for four types of projectile. Data on aerodynamics and dynamics of flight for fragments are presented. Cha1026racterization of Held's constants was performed, and prediction of initial fragment velocities, and lethal zones for four types of projectile was made.

2 Theoretical background

2.1 Number and mass distribution of fragments

Most of the research of high explosive projectile natural fragmentation is pointed towards detonating cylindrical metal rings, which implies that rarely projectile real geometry is taken into account when investigating number and mass distribution of fragments.

Overview of literature regarding mass distribution of fragments leads to conclusion that Mott, Gurney-Sarmousakis and Held formulas are the most used methods in determination of fragment mass distribution laws. There are alternatives to these methods, such as Magis, Randers-Pehrson, Stromse-Ingebritsen methods. Also, currently popular methods are Grady model, as well as Gold methodology [5, 6, 7, 8, 9, 10, 11, 12, 13, 14].

Mott's expression for average fragment mass μ is:

$$\mu = B_M{}^2 \cdot t^{5/3} \cdot d_i^{2/3} \cdot \left(1 + \frac{t}{d_i}\right)^2 \qquad (2.1.1)$$

where: B_M - Mott's constant, t - projectile body thickness, d_i - explosive diameter.

Gurney-Sarmousakis formula for assessment of average fragment mass is:

$$\mu = A_{G-S}{}^2 \cdot \left(\frac{t}{d_i}\right)^2 \cdot (d_i + t)^3 \cdot \left(1 + \frac{C}{2M}\right) \qquad (2.1.2)$$

In (2.1.2) $\mu = m_f/j$ (average fragment mass generally depends on dimensionality of process), m_f - fragment mass, j - dimensionality (for C/M < 2 j = 2, and for C/M > 2 j = 1), C - explosive mass, M - projectile body mass, A_{G-S} - Gurney-Sarmousakis constant (as an approximation $A_{G-S} = 338{,}1/P_{det}$, where P_{det} is detonation pressure of explosive used).

Gold and Baker developed following method for assessment of average fragment mass:

$$\mu = \sqrt{\frac{2}{\rho_f}} \cdot \left(\frac{\sigma_v}{\gamma_M}\right)^{3/2} \cdot \left(\frac{r_i}{v_r}\right)^3 \qquad (2.1.3)$$

where: r_i - explosive charge radius, v_r – radial expansion velocity of projectile body , ρ_f – density of fragment material, σ_v – yield strength of projectile body material, γ_M –empirical Mott's constant (characteristics of material in dynamic fracture conditions).

Grady and Kipp determined average fragment mass through an expression:

$$\mu = A_G \cdot \rho_f \cdot t^3 \cdot \left(\frac{R_0}{t}\right)^{2s_G/\alpha_G} \cdot \left(\frac{G_G/t^{2-\alpha_G}}{\rho_f \cdot V_r^2}\right)^{s_G/\alpha_G} \qquad (2.1.4)$$

where A_G – length to width ratio for fragment, R_0 – nominal radius of projectile, s_G - constant (2 or 3, depending on fragment thickness), α_G - constant ($2 \leq \alpha_G \leq 3$), G_G – fracture resistance of material (determined through Kipp-Grady energy methodology or Mott statistical method).

For prediction of mass of fragments, Held developed method, based on optimization of empirical constants through regression analysis, where largest fragment are discarded:

$$m = \frac{dM(n)}{dn} = M_0 \cdot B \cdot \lambda \cdot n^{\lambda-1} \cdot e^{-Bn^\lambda} \qquad (2.1.5)$$

$$M(n) = M_0\left(1 - e^{-B \cdot n^\lambda}\right) \qquad (2.1.6)$$

In Held's expressions (2.1.5) i (2.1.6): m – mass of fragments as a function of cumulative fragment number, M(n) - cumulative fragment mass, M_0 – total mass of collected fragments, n - cumulative fragment number, B and λ = Held's constants ($B \approx 0{,}01$; $\lambda \approx 0{,}75$).

Methodologies for prediction of fragments number [6, 7, 15, 16, 8, 17] are based on general form:

$$N(m) = N_0 \cdot e^{-\left(\frac{m}{\mu}\right)^{\beta}}$$

(2.1.8)

where: N(m) - cumulative fragments number (fragment number with mass larger than mass m), N_0 - total number of fragments, μ - average fragment mass determined through one of the methods mentioned earlier, β - constant (measure of fragment size dispersion).

Mott's expressions for assessment of fragments number for 2D and 3D cases are:

$$N(m) = N_0 \cdot e^{-\left(\frac{m}{\mu}\right)^{1/2}} \text{ - for 2D case and } N(m) = N_0 \cdot e^{-\left(\frac{m}{\mu}\right)^{1/3}} \text{ - for 3D case} \quad (2.1.9)$$

where: N_0 = M/2μ (for 2D case), and N_0 = M/6μ (for 3D case), M – total mass of projectile body, 2μ - average fragment mass for 2D case, and 6μ - average fragment mass for 3D case.

According to Grady-Kipp model, constant β = 1 (but can be empirically determined using regression analysis of test data):

$$N(m) = N_0 \cdot e^{-\left(\frac{m}{\mu}\right)}$$

(2.1.10)

Grady-Kipp formula for predicting bilinear distribution is:

$$N(m) = f_1 \cdot e^{-\frac{m}{\mu_1}} + (1 - f_1) \cdot e^{-\frac{m}{\mu_2}}$$

(2.1.11)

where: f_1, f_2 - parameters of bilinear distribution (obtained by solving system of four nonlinear equations), μ_1, μ_2 - average fragment mass for different mass domains.

2.2   Aerodynamics and dynamics of flight for fragments

There are only few studies dealing with research of fragment aerodynamics, and generally there are no publicly available data on fragment drag coefficient.

During the flight of fragment through the air, drag force slows down the fragment. This force is a function of fragment velocity V, air density ρ, exposed area of fragment A and non-dimensional drag coefficient C_D:

$$F_D = \frac{1}{2} A \rho C_D V^2$$

(2.2.1)

Aerodynamic drag coefficient depends largely on fragment shape and Mach number. Influence of Reynlods number can be neglected because of fragment thumbling and its irregular surface with many sharp edges.

Non uniformity of fragment shapes poses a significant problem in prediction of its aerodynamic drag coefficient.

In vertical tunel experiment [1], 58 fragments were collected out of several simultaneous detonations of projectile 155mm, and fragments were divided into five characteristic shapes. There was a subsonic drag coefficient to fragment shape correlation.

In second experimental program [2], approximately 100 fragments were tested at Mach numbers ranging from 0.67 to 3.66. Fragments were divided into nine different shapes and again the correlation between drag coefficient and fragment shape was evident. Only 11 fragments were tested in subsonic condition and the C_D varied from 0.68 to 1.61. Supersonic C_D varied from 0.76 to 2.98.

COPPER BAND	BOX PLATEAU	PARALLEL PIPED	MOUNTAIN RIDGE	WEDGES
Smooth, rounded surface, flat bottom	Large portion of both sides is flat, flat sections are smooth, no general overall shape	Large portions of both side are flat and smooth, overall rectangular shape	Flat bottom, forms a ridge a top	Triangular shape, two of the three surfaces are generally smooth
C_D = 1.11 to 1.44	C_D = 1.211 to 1.59	C_D = 1.34 to 2.07	C_D = 0.65 to 1.39	C_D = 0.618 to 1.01

Figure 1: Characteristic fragment shapes [1,3]

By combination of these two experimental programs, curves of minimal, maximal and average drag coefficient vs Mach number were made (fig. 2). It is assumed that at least 95% of all fragments will have drag coefficient between minimal and maximal values in fig. 2 [3].

Tests are showed that fragment of elongated shape tries to position itself in such a state in which its largest area of cross section is normal to fragment flight direction.
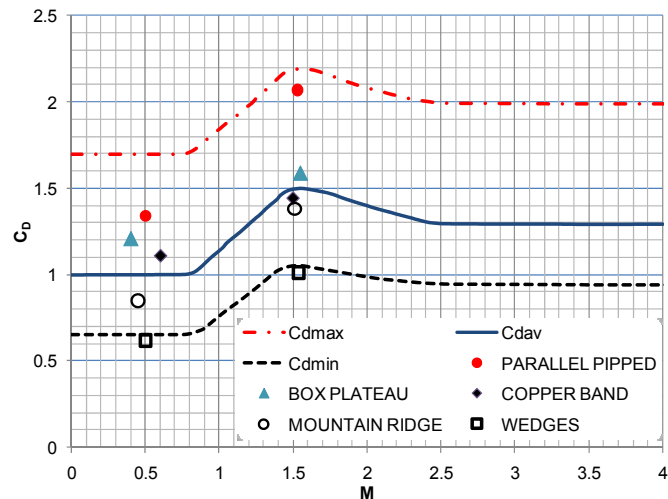

Figure 2: Drag coefficient vs. Mach number [1,3]

According to DDESB (Department of Defense Explosives Safety Board), minimal kinetic energy of fragment E_{KS} needed for incapacitation of soft target (ie. soldier) is 80J, so minimal fragment velocity, based on the criteria, can be written as:

$$v_{min} = \sqrt{\frac{2E_{KS}}{m}} \qquad (2.2.2)$$

Expression (2.2.2) enables an assessment of efficient fragment distance (distance on which fragment is capable of human target incapacitation).

Trajectory of fragment moving under the influence of drag and gravity force can be determined using point mass trajectory model:

$$m\frac{d^2x}{dt^2} = -\frac{A\rho C_D}{2}V\frac{dx}{dt} \qquad (2.2.3)$$

$$m\frac{d^2y}{dt^2} = -\frac{A\rho C_D}{2}V\frac{dy}{dt} - mg \qquad (2.2.4)$$

$$m\frac{d^2z}{dt^2} = -\frac{A\rho C_D}{2}V\frac{dz}{dt} \qquad (2.2.5)$$

With expressions (2.2.3) - (2.2.5), three additional kinematic equations and known initial conditions are used, assuming knowledge of drag law $C_D = C_D(M)$.

In reality, in analysis of warhead lethal zone, velocities of largest number of fragments are supersonic.

3   Research and analysis of results

Parameters of natural fragmentation process are determined with analytical methods, experimental researches and numerical modeling methods. Number of fragments, their mass, geometrical shapes and spatial distribution are determined experimentally, using Pit and Arena test methods. In Pit test, warhead is detonated in closed space, filled with sand. After the fragmentation of warhead, fragments are collected from the sand. Mass and shape of fragments are determined, and fragments are classified by their mass groups. Spatial fragments distributions were determined through Arena tests. In the arena fragmentation test, fragments concentration density is measured when projectile is in vertical position on the ground.

Trend in the world is design of munition with advanced performances, range, lethality, design (ratios t/d and C/M – more explosive mass C, smaller case thickness, slenderer projectiles, safety in launch phases is higher by using materials with better mechanical characteristics). Higher projectile range brings the need for slenderer weapon barrels (up to 57 calibers), higher pressures in the weapon barrel and accordingly need for better material performances of projectile body. Optimization of parameters of structural resistance of projectile body during the launch phase, and parameters of projectile terminal ballistics, remains complex problem.

3.1   Characteristics of projectile body material

Depending on projectile type, different metals are used for manufacturing of projectile body (carbon steel, carbon steel alloys with high percentage of tungsten). Most of these materials were developed for specific projectile to ensure safety in launch and high efficiency.

Around the world there are big differences in production technologies, which have a significant influence to munition quality. Authors were researching several types of projectile body materials used in USA, Russia and former Yugoslavia.

Currently mostly used steel for US HE projectiles is HF-1 steel, which is used to produce projectiles 155-mm M549 RAP, 155-mm HE M795, and 203mm M650, RAP, and it is being considered for other HE projectiles. The required mechanical properties are: 965 MPa yield strength and 5% minimum elongation [22].

Russians for calibers from 76mm to 152mm use following rolled steels for projectile bodies: S-55, S-60 and 45Kh1 [23].

In former Yugoslavia our own technologies were adopted for manufacturing projectile bodies. Steels used primarily for projectile bodies were Č.1534VP, Č.1737VP, Č.1635VP, Č.9180VP and Č.4135VP.

Table 1: Mechanical characteristics of steel materials

Material JUS/DIN	Projectile	Mechanical characteristics								
		Minimal requirements				Measured values				
		R_v [MPa]	R_m [MPa]	δ [%]	ψ [%]	R_v [MPa]	R_m [MPa]	R_m/R_v	δ [%]	ψ [%]
Č.1543VP/ C45G	120 mm, HE, M62P3	324	588,6	15	-	325,5 - 463,6	636 - 796,1	1,62 2,28	16,2 27,5	-
Č.1635VP / DIN 17200	105 mm, HE, M1	448.3	-	15	30	448,4 - 579,.5	684,1 909,7	1,43 1,73	17,1 26	32,6 - 63,8
Č.1737VP	82 mm, HE, M74	-	-	-	-	441- 549	731- 837	-	20- 22,5	-
	122 mm, OF-462	323,7	-	-	15	330,1 - 434	713,4 - 884,6	1,92 - 2,23	13 - 18,6	19,8 - 32,9
	130 mm, HE, M79	313,9	-	-	15	321,6 - 486	737,3 - 927,2	1,91 - 2,31	12 - 16	16,9 - 24,6
Č.9180VP	105 mm, HE, M1	448,3	-	15	30	451 - 604,5	692 - 856,6	1,27 - 1,64	16,1 - 24	31,3 - 51,4

In table 1 mechanical characteristics of steel used in our country were presented for several types of projectiles, as well as measured mechanical characteristics. Yield strength is denoted as R_v, tensile strength as R_m, elongation as δ, and contraction as ψ.

It is important to notice that after thermal treatment mechanical characteristics of materials are considerably improved, compared to ones defined in standards.

Average value of tensile strength for mortar projectile 120 mm, HE, M62P3 (Č.1543VP), is 727,75 MPa, which is 23,6% larger (fig. 3) than minimal allowable value according to standard.
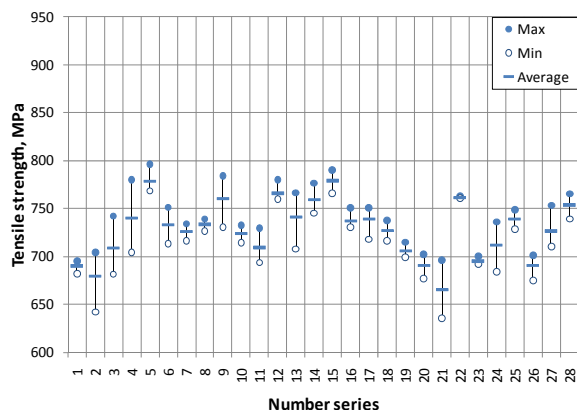
Figure 3: Variation of tensile strength values for different mechanical series for mortar projectile 120 mm, HE, M62P3
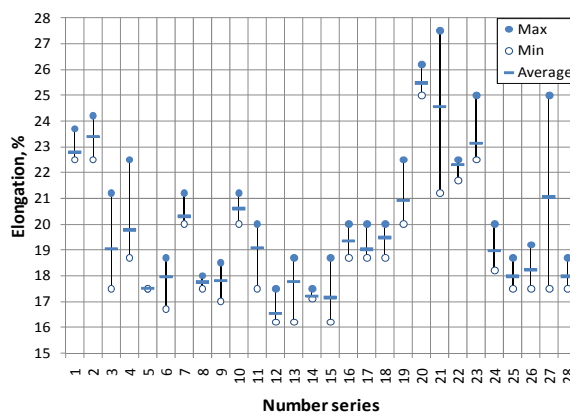
Figure 4: Variation of elongation values for different mechanical series for mortar projectile 120 mm, HE, M62P3

Tensile strength values for projectile 105mm, HE, M1 are in the range from 692 to 856.6 MPa for Č.9180VP, and for Č.1635VP in the range from 684 to 910 MPa (fig. 5). Average value of tensile strength for Č.1635VP is 2,5% larger than for material Č.9180VP.

Change of demands for mechanical charactersitics of metarials (instead of elongation parameter now contraction is used) has been conducted (fig. 6). Average value of contraction for material Č.9180VP is for 32% larger than demanded, and for Č.1635VP around 76,5%.
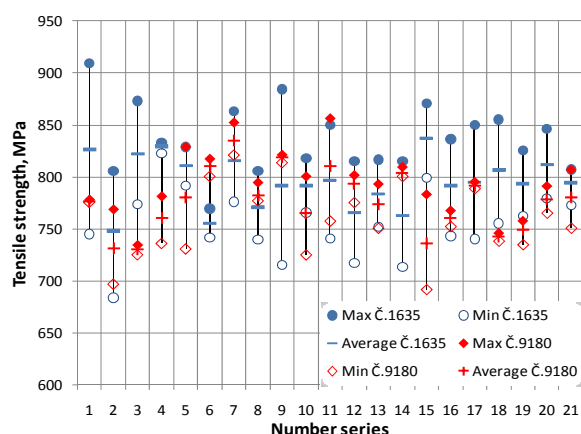
Figure 5: Variation of tensile strength values for different mechanical series for 105 mm, HE, M1, and for materials Č.9180VP and Č.1635VP
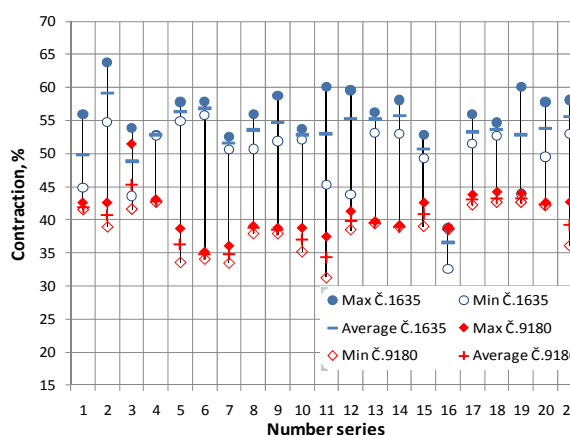
Figure 6: Variation of contraction values for different mechanical series for 105 mm, HE, M1, for materials Č.9180VP and Č.1635VP

Average value of tensile strength for 130 mm, HE, M79 is 3% larger than for projectile 122 mm, OF-462 (fig. 7). Contraction parameter values for this material and both projectiles are 50% less than demanded for projectile 105mm M1. Average value of parameter contraction for projectile 122 mm, OF-462 is around 65% larger than demanded in standard, while for 130 mm, HE, M79 this values are around 37,7% higher (fig. 8).
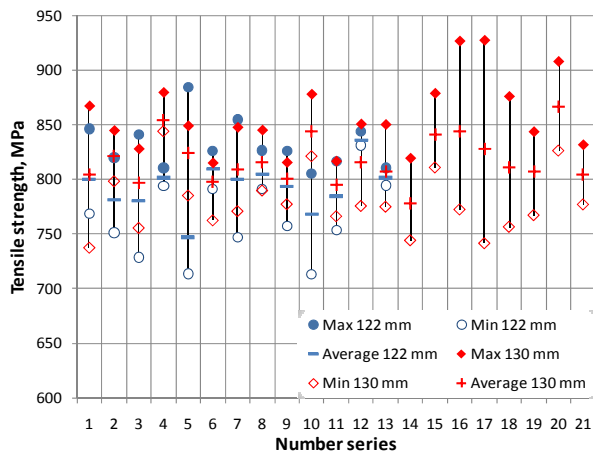
Figure 7: Variation of tensile strength values for material Č.1737VP for mechanical series of 122mm OF-462 and 130 mm, HE, M79
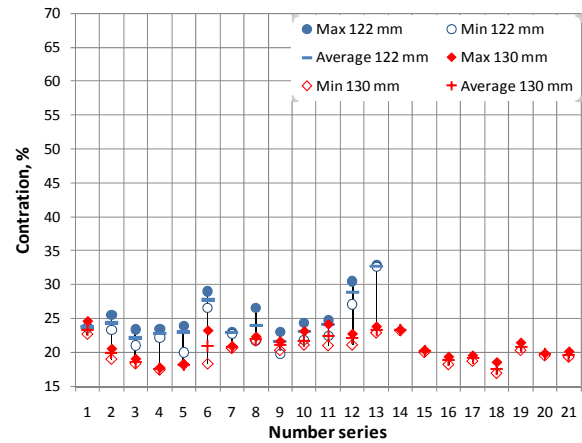
Figure 8: Variation of contraction values for material Č.1737VP for mechanical series of 122mm OF-462 and n 130 mm, HE, M79

Proces of thermal treatment of material (table 1) is very important for mechanical performances and character of fragmentation process. In most of available publications this fact is rarely highlighted. Body of projectiles made from thermally treated steels (ie. US HF-1 steel) generally have more uniform distribution of shapes and mass of fragments, and this is important fact when terminal ballistics parameters of high explosive projectiles are considered.

3.2   Fragment mass distribution

In the research authors analyzed mass distribution of fragments using Held methodology and the results are compared with experimental Pit tests. Through analysis of test data, range of Held's parameters B and λ was determined. Expressions (2.1.5) and (2.1.6) were used for prediction of fragment mass m as a function of cumulative fragments number n.

Accordingly, ratio C/m (explosive mass to case mass) was determined for all tested projectiles, as well as nondimensional geometrical ratio t/d, where t - equivalent body thickness and d - equivalent explosive diameter, determined from known explosive mass and volume. Equivalent body thickness was determined using:

$$V_c = \frac{D^2 - d^2}{4} \cdot \pi \cdot L_{\exp} \tag{3.1.1}$$

$$t = \frac{1}{2}\left[\sqrt{d^2 + \frac{4V_c}{\pi \cdot L_{\exp}}} - d\right] \tag{3.1.2}$$

where V_c - volume of projectile body over explosive length $L_{\exp}$ and D - equivalent diameter of projectile (determined through d, V_c and $L_{\exp}$).

Analysis of fragmentation parameters for four projectile types was performed, after the fragmentation in Pit tests. Projectiles 120 mm HE, M62P3, (120 pieces) 105 mm, HE, M1 (8 pieces), 122 mm, OF-462 (8 pieces) and 130 mm HE, M79 (3 pieces) were tested.

Held diagrams, where mass of fragments is presented as a function of cumulative fragments number, are shown in fig. 9, for four different types of projectiles.

During the determination of Held's constants B i λ, large fragments (mass over 100g) were neglected. Better correlation was achieved (correlation coefficient over 0,99) using this technique.
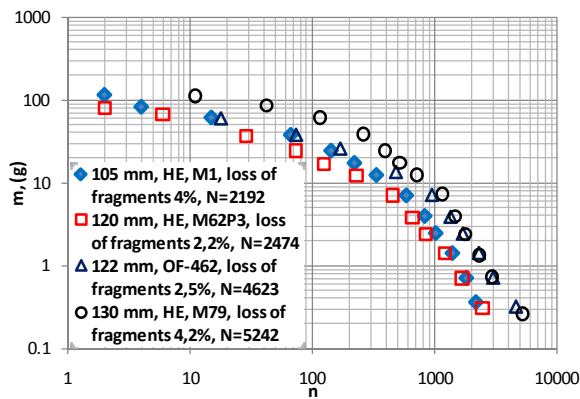
Figure 9: Mass of fragments vs. cumulative fragments number (TNT explosive charge)
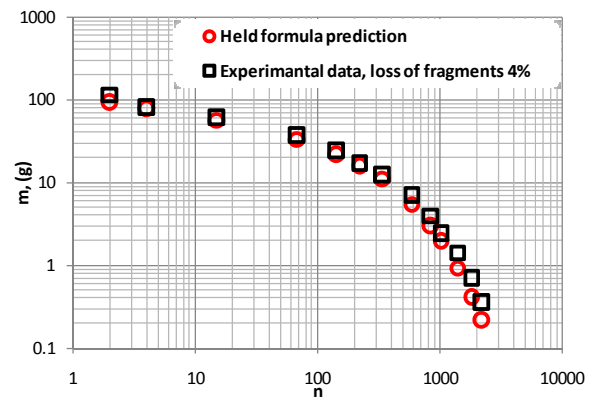

Figure 10: Comparation of Held prediction and experimental data for projectile 105mm, HE, M1 (TNT)

Diagram in fig. 10 shows generally good agreement of Held method with experimental data. Somewhat poorer agreement of data was noticed for smaller mass groups, as a result of applied technology for fragments collection. Technique of fragment collecting in Pit test influences the number of obtained fragments. In Pit tests where fragments are collected using magnets, number of recovered fragments with smaller mass will be higher, comparing to manual technique of fragment recovery.

Table 2: Values of Held's constants B and λ for tested projectiles

Projectile	Loss of fragments mass	B	λ	R^2	t/d	C/m
105mm, HE, M1, TNT	4,0 %	0,0110	0,7835	0,9993	0,191	0,222
120mm, HE, M62P3, TNT	2,2 %	0,0121	0,7641	0,9990	0,151	0,290
122mm, OF-462, TNT	2,5 %	0,0065	0,7866	0,9984	0,185	0,225
130mm, HE, M79, TNT	4,2 %	0,0070	0,8033	0,9978	0,258	0,158

Held's constants B i λ, non dimensional ratios t/D (geometric ratio) i C/m (mass ratio), and loss of fragment mass during fragmentation Pit test are shown in table 2.

Table 2 shows that The difference in parameter B for four tested projectiles was around 40% for tested projectiles, while constant λ differed by 5%. This leads to conclusion that constant B is more sensitive than constant λ, which is in accordance with our previous work [18].

Simulation of influence of change of parameter B for ±10%, while λ = const, and change of parameter λ for ±10%, while B = const, was performed. Simulation showed that mass distribution laws are more sensitive to change of λ than to change of parameter B. (fig. 11 and 12).
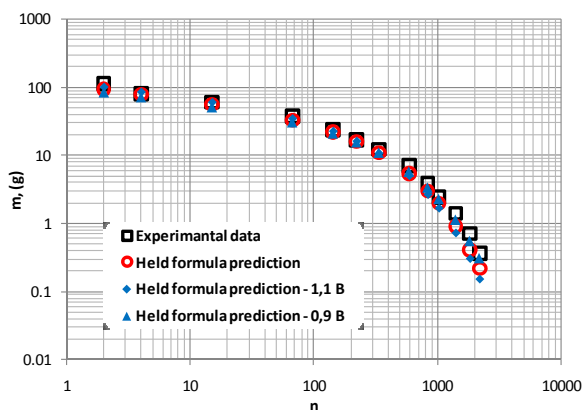

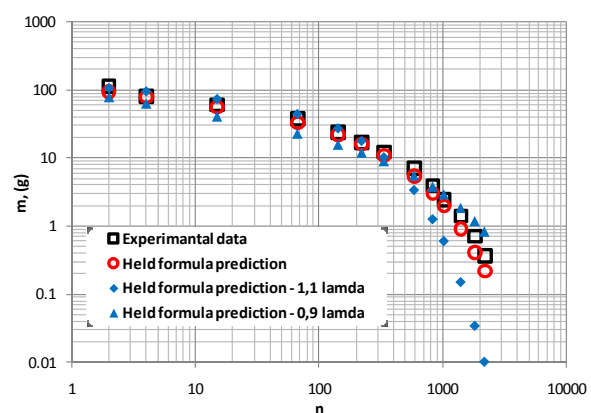**Figure 11:** Influence of change of parameter B for ±10% (λ=const) for 105 mm, HE, M1

Figure 12: Influence of change of parameter λ for ±10% (B=const) for 105mm, HE, M1

Also, analysis showed when fragments with mass over 100g were included in consideration (usually up to 10 fragments), values of B parameter was significantly decreased and values of parameter λ were increased (ie. for projectile 105 mm, HE, M1 value of B dropped by 24%, and value of λ increased by 5%).

On the other side, higher number of collected fragments under 0,5 g resulted in an increase of coefficient B, and decrease of λ (ie. for projectile 105 mm, HE, M1 value of B jumped by 4%, and value of λ dropped by 3%).

Held method is useful for preliminary analysis, but with diagrams in fig. 9 and 10 it is generally difficult to derive certain conclusions regarding influence of parameters on fragmentation process.

Authors proposed [18,19] a method for visualization of test data as a mean of assessment of influence of individual parameters on mass distribution. As an independent value mass of individual fragment group was taken. Correlation is established between number of fragments whose masses were smaller than average fragment masses and total number of fragments (N_i/N for $m_i < m_{aver}$), and also between masses of these groups and total mass of fragments (M_i/M for $m_i < m_{aver}$). This is shown in figures 13 and 14.
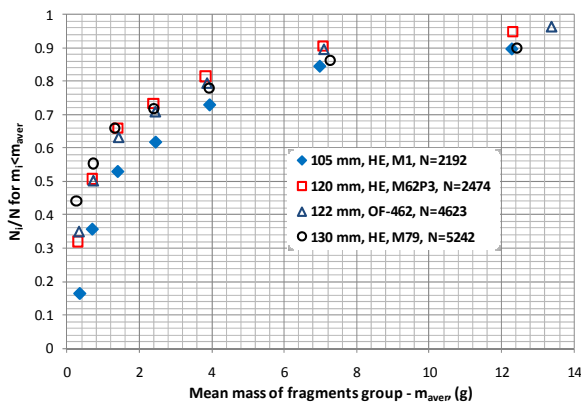

Figure 13: N_i/N for $m_i < m_{aver}$ vs m_{aver} for four different types of projectiles
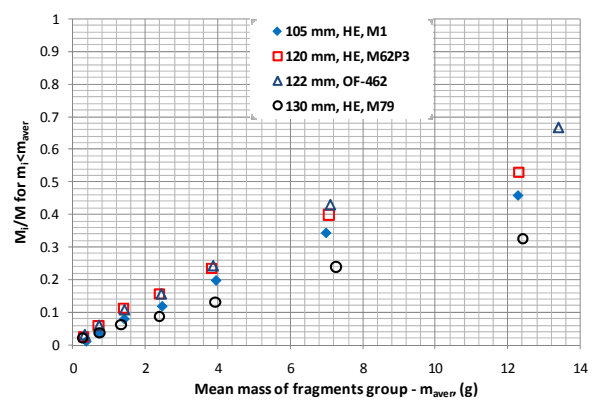
Figure 14: M_i/M for $m_i < m_{aver}$ vs m_{aver} for four different types of projectiles

In fig. 13 and 14, diagrams of N_i/N for $m_i < m_{aver}$ vs m_{aver}, as well as M_i/M for $m_i < m_{aver}$ vs m_{aver} for four different types of projectiles are presented.

From fig. 13 it can be concluded ie. that 80% of all fragments have mass smaller than 5g. This conclusion is very important, since in some publications, authors focus mostly on larger fragments.

Also, from diagram in fig. 14 it can be seen that fragments with mass smaller than 5g make for around 25% of total fragments mass.

Fragments with mass from 5 to 10 g make for around 10% of total fragment number, and around 25% of total fragment mass. While fragments with mass larger than 10 g make for 10% of total fragment number and around 50% of fragment mass..

3.3 Lethal efficiency

Analysis of initial fragment velocity was performed using Gurney methodology [18, 20]. Using CAD methods and Gurney formula, theoretical assessment of initial fragment velocity was made as a function of reletive position of projectile body segments, for four different projectile types.

Fig. 15 shows that mortar projectile 120mm M62P3 has highest theoretical initial fragment velocity (maximum around 1250 m/s). Following projectile is 105mm M1, and than 122mm

OF-462. Projectile 130mm M79 has the lowest initial fragment velocity, whose fragment velocities in central segments are not higher than 1000 m/s.

If a nondimensional ratios t/d and C/m (fig. 15) are reviewed for tested projectiles, conclusion arises that projectile 120mm M62P3 has highest value of ratio C/m and lowest value of ratio t/d.
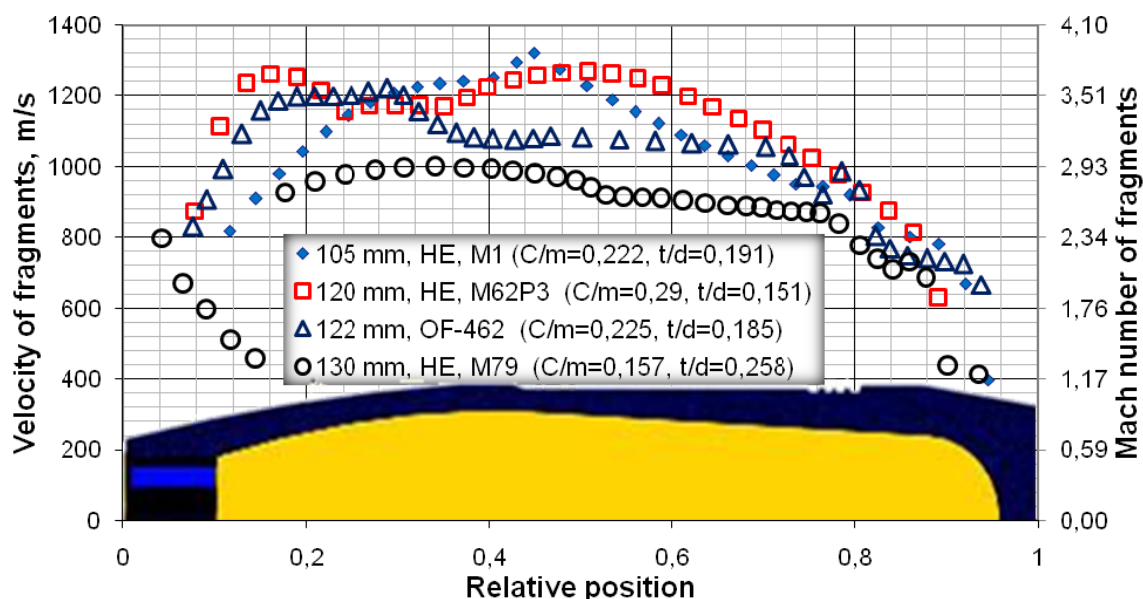

Figure 15: Initial velocities of fragments for four different types of projectiles (explosive TNT)

Change of fragment velocity on trajectory as a function of range (fig. 16) was determined by using point mass trajectory model. Complex shape of fragment was approximated with parallelepiped shape of equivalent mass. Dimmensions of fragment were *a* x *a* x 3*a*.

Average exposed area of fragment was determined using accomodation factor for given fragment shape. Fragment accomodation factor was determined analytically, based on fragment dimensions and density of fragment material [21].

Differential equations of fragment motion were numerically solved using Runge-Kutta method of fourth order.

Change of fragment velocity on trajectory as a function of range was considered for fragments with masses from 0.5 to 10 g, where for every fragment three different range calculations were made, with C_{Dmin}, C_{Dav} and C_{Dmax} (fig. 2). For clearer diagram in fig. 16, only 7 curves were presented (for fragments with masses 0.5 and 10 g with drag laws C_{Dmin}, C_{Dav} and C_{Dmax}, and for fragment mass 2.5 g for which drag law change was according to $C_{Dav}=f(M)$ from fig. 2).

From diagram in fig. 16 it is clear that character of velocity change primarily depends on shape and mass of fragments, and can be generally similar for different fragment masses.
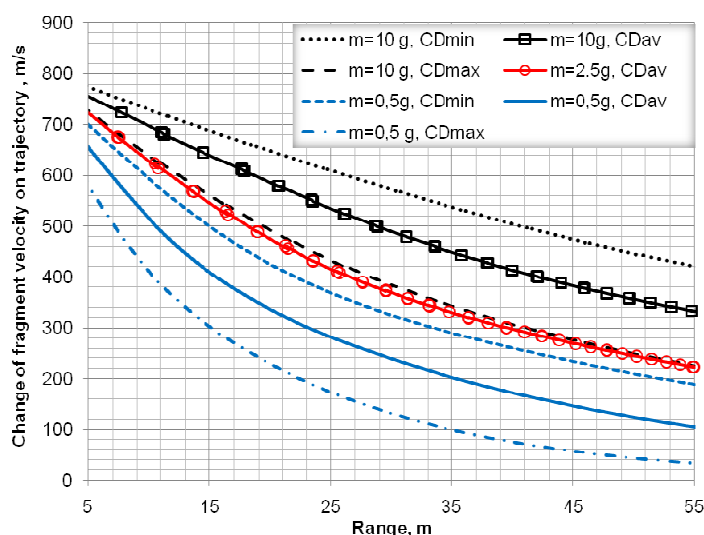

Figure 16: Change of fragment velocity on trajectory as a function of range

Assessment of velocity on trajectory for fragment with mass of 10g and C_{Dmax} is almost identical as an assessment of velocity on trajectory for fragment with mass of 2,5g and C_{Dav}. This clearly shows an influence of fragment shape on projectile lethal zone.

Based on minimal kinetic energy of fragment needed for inacapacitation of soldier, range of efficient fragments was determined as a function of fragment mass (fig. 17), where it was assumed that drag coefficient changes as a function of Mach number by laws showed in fig. 2 [3].
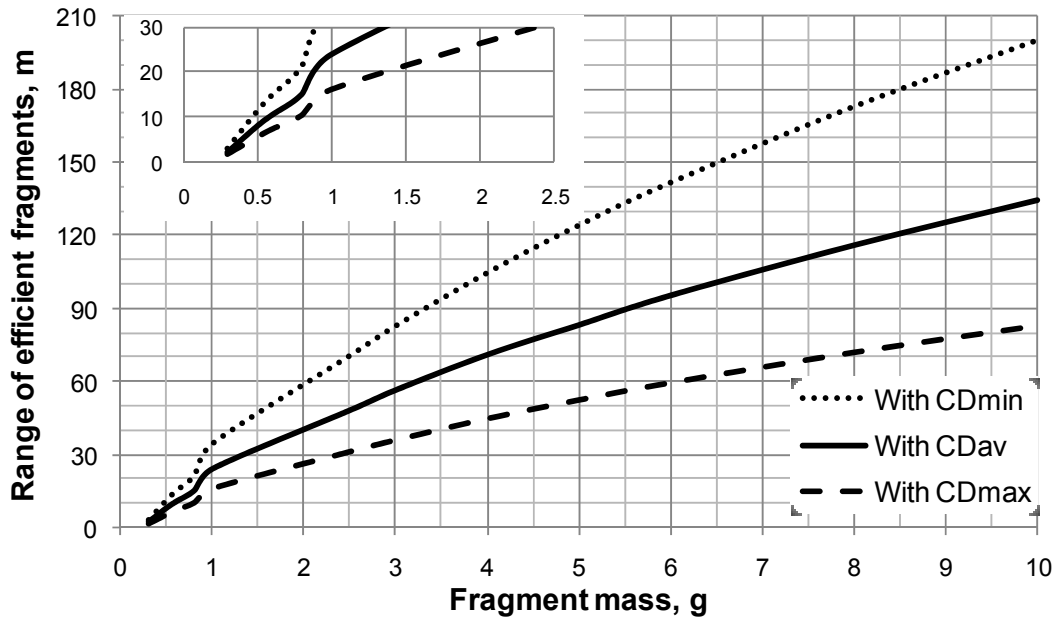

Figure 17: Range of efficient fragments for HE projectile 130 mm M79 [1,3]

From fig. 17 it is clearly shown that fragments with masses up to 3 g for projectile 130mm M79 can have an efficient range from 32m up to 85 m, depending on their shape, or depending on drag law for moving fragment.

If drag coefficient is assumed to be constant (zone of supersonic velocities), an assessment of efficient range of fragment can be made using:

$$X_{ef} = \frac{2m}{C_D A \rho} \ln \frac{V_0}{\sqrt{\frac{2E_{KS}}{m}}} \tag{3.2.1}$$

In (3.2.1) m is fragment mass, A - exposed area of fragment, ρ - air density and V_0 - initial velocity of fragments.

Differences in effective ranges (for sphericaly shaped fragments) from different mass groups, determined using relation 3.2.1, with an assumption of supersonic drag coefficient $C_D=1,3$ and by using point mass trajectory model with drag law $C_{Dav}= f(M)$ for real fragments are not higher than 5% for initial velocity of fragments higher than 800 m/s.

Zone of lethal efficiency was determined in in quarter-circular Arena. Results of the experiment are analised for two projectiles 120 mm, HE, M62P3, eight projectiles105 mm, HE, M1, six projectiles 122 mm, OF-462 and two projectiles130 mm HE, M79.

Projectiles were made to stand verticaly with their fuses pointing to the ground. Quarter-circular wooden panels, 25,4 mm thick and 2 m high, were positioned on different distances from explosion center (10 m, 15 m, 20 m and 30 m). Fragments that penetrated wooden panels and fragments that hit (but not penetrated) panels were registered on all four distances in Arena.

Diagram in fig. 18 shows density of efficient fragment as a function of detonation distance for four considered projectiles.

Projectile 130mm, HE, M79 has highest lethality radius, followed by projectile 122 mm, OF-462, then projectile 105 mm, HE, M1 and then has mortar projectile 120mm, HE, M62P3 with lowest lethality radius ($\text{Ref}_{120mm} = 17$ m, $\text{Ref}_{105mm} = 17,3$ m, $\text{Ref}_{122mm} = 23,8$ m i $\text{Ref}_{130mm} = 27,1$ m).
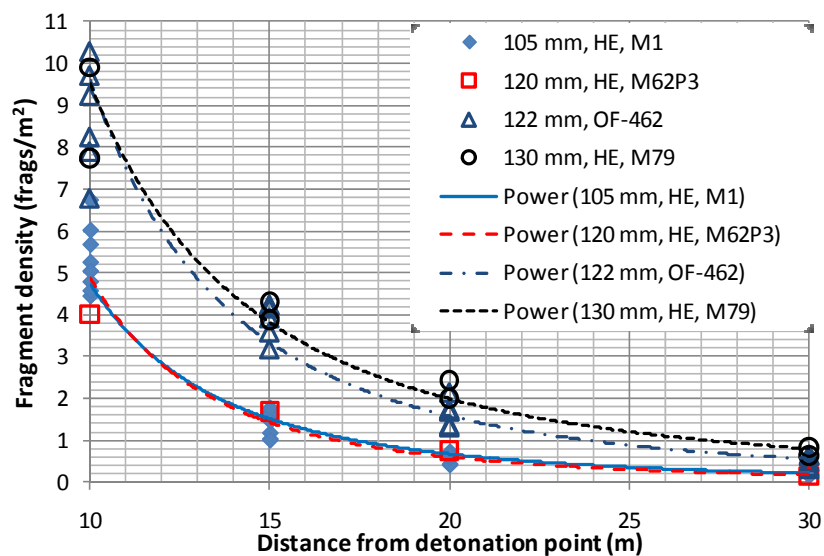

Figure 18: Efficient fragment density vs. distance for four different types of projectiles

Comparation was performed for Pit tests data (number and mass of fragments by individual groups) and for Arena tests data (number of perforation and hits in wooden panels on four distances from explosion center.
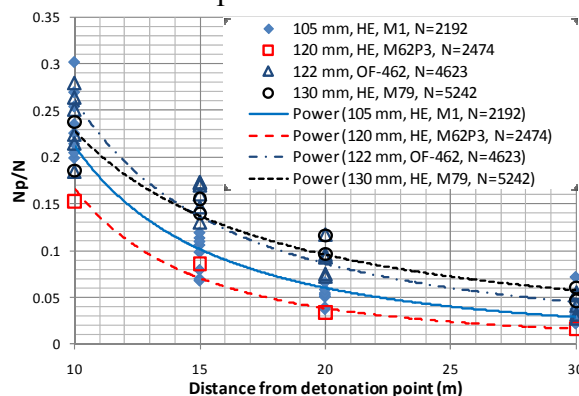

Figure 19: Efficient fragment density/total number of frag. vs. distance for four types of projectiles
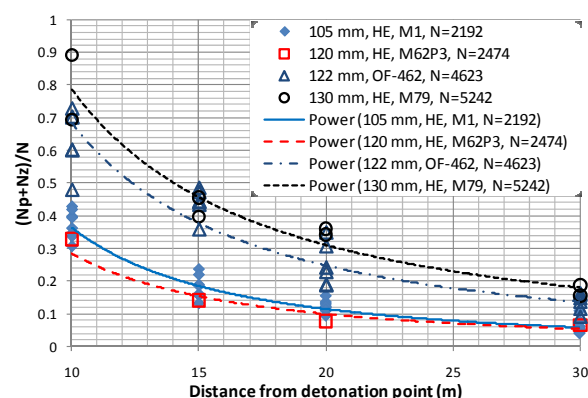

Figure 20: Fragment density/total number of frag. vs. distance

Comparison of fragment number N, determined using Pit tests, number of fragments penetrating wooden quarter-circular panels N_p, and number of fragments partially penetrating wooden quarter-circular panels N_z, during Arena tests, were made. The goal was to make an assessment of ratio of efficient fragments N_p ($EK \geq 80J$) and active fragments ($N_p + N_z$) that hit vertical quarter-circular wooden panels, 2m high, on different distances from explosion (fig. 19 and 20).

Analysis showed that for mortar projectile 120 mm, HE, M62P3 on distance of 17 m, only 5,5% of efficient fragments (N_p/N) were registered and around 11,5% of active fragments (($N_p+N_z)/N$), while for projectile 130mm, HE, M79, on distance of 27m from explosion center, there were around 6,5% of total number of efficient fragments, and around 20% of total active fragments.

On distance of 10m from the explosion, mortar projectile 120 mm, HE, M62P3, has around 15% of efficient fragments, and around 30% of active fragments.

4   Conclusions

Types of material for projectile body, applied thermal treatment, uniformity of manufacturing process for projectile body, behaviour of material in dynamic conditions significantly influence the shape and number of fragments.

Analysis of mechanical characteristics of projectile body materials for series from several years, with total quantity around 300 000 ammunition pieces, showed that mechanical characteristics significantly changes with mechanical series, and this surely influences the number, mass and shape of fragments.

Analysis of fragment mass distribution using Held method, where largest fragments were neglected, showed excellent correlation with experiments. During analysis of four types of projectiles, it was noticed that value of Held's constant B varied up to 40%, while constant λ varied only by 5%. This leads to conclusion that constant B is more sensitive than constant λ, which is consistent with our previous work. In further analysis it was determined that, while λ=const, an influence of parameter B is insignificant for Held mass distribution law, while with B=const, parameter λ significantly influenced the character of Held's mass distribution law, especially in zones with smaller mass groups.

Authors proposed method that enables more precise analysis of influence of individual parameters (explosive mass, type of explosive and body material, influence of body shape, etc) on process of natural fragmentation.

By analyzing fragmentation parameters of four considered projectiles, it was noticed that around 80% of all fragments have masses smaller than 5g, and that these fragments comprise around 25% of total fragment mass. Fragments with mass from 5 to 10 g make for around 10% of total fragments number, or 25% of total fragments mass, while fragments with mass larger than 10g make for remaining 10% of total fragments number and around 50% of total fragments mass.

Analysis of fragment flight dynamics for minimal effective kinetic energy of fragment, needed for soldier incapacitation for different mass groups, showed high influence of fragment shape (fragment drag law) to exterior ballistic properties of fragment and thus to lethality zone of projectile.

Lethality radius is influenced by number of fragments, fragment mass distribution, shape of fragment (fragment drag), fragment velocity, external and internal shape of projectile body, material type of projectile body and explosive charge, applied thermal treatment for body material, explosive chain in projectile, etc

Based on analysis of fragmentation parameters in Pit and Arena tests for four projectiles considered, authors concluded that from total number of fragments formed made during explosion, only 11,5% to 20% fragments hit wooden panel (height 2 m, thickness 25,4 mm) on distance considered as lethality radius, of which only 5,5% to 8% possess enough (minimal) kinetic energy of 80J, needed for incapacitation of soft targets.

5   References

[1] N. J. Moga and K. M. Kisielewski, Vertical wind tunnel tests to determine subsonic drag characteristics of unscored warhead fragments, NSWC TR 79-112, Dahlgren, Virginia, May 1979.
[2] J. W. McDonald, Bomb fragments, Eglin Air Force Base, 23 September 1980.
[3] J. G. Powell, W. D. Smith, F. McCleskey, Fragment hazard investigation program: natural communication detonation of 155-mm projectile, NSWC TR 81-54, Dahlgren, Virginia, July 1981.
[4] F. McCleskey, Drag coefficients for irregular fragments, NSWC TR 87-89, Dahlgren, Virginia, February 1988.
[5] J. Carleone: Tactical Missile Warheads, Progress in Astronautics and Aeronautics, Volume 155, AIAA, 1993.

[6] Victor: Warheads performance calculations for threat hazard assessment, Victor Technology, San Rafel, California.

[7] V. M. Gold, Engineering model for design of explosive fragmentation munitions, US Army AR-DEC, AETC, Picatinny Arsenal, NJ, february 2007.

[8] J. Hokanson, Fragment and debris hazards from accidental explosions, Naval Surface Weapons Center, Dahlgren VA, 13 july 1981.

[9] V. Gold, E. Baker, K. Ng, J. Hirlinger, New Methodology for Simulating Fragmentation Munitions, US Army, TACOM-ARDEC, Picatiny Arsenal NJ.

[10] V. Gold, E. Baker, W. Poulos, Modeling Fragmentation Performance of Natural and Controlled Fragmentation Munitions, 23rd International Symposium on Ballistics, Tarragona, Spain, 16-20 april 2007.

[11] V. M. Gold, E. L. Baker, W. J. Poulos, B. E. Fuchs, PAFRAG modeling of explosive fragmentation munitions performance, International Journal of Impact Engineering 33, 294–304, 2006.

[12] M. Held, Fragment Mass Distribution of Debris, Minutes of the Explosives Safety Seminar (24th) Held in St. Louis, MO, 28-30 August 1990.

[13] V. M. Gold, Y. Wu, Modeling Fragmentation Performance of Insensitive Explosive Fragmentation Munitions, 2009 Insensitive Munitions and Energetic Materials Technology Symposium, Tucson, Arizona, 11-14 May 2009.

[14] Structures to resist the effects of accidental explosions, fragment and shock loads, Army TM 5-1300, Navy NAVFAC P-397, Air Force AFR 88-22, 1990.

[15] D. R. Curran, J. D. Colton, Improved Fragmentation Algorithms for Debris Environments, Defense Nuclear Agency, Alexandra VA, September 1996.

[16] D. Grady, L. Wilson, D. Reedal, D. Kuhns, M. Kipp, J. Black, Comparing alternate approaches in the scaling of naturally fragmenting munitions, 19rd International Symposium on Ballistics, Interlaken, Switzerland, 7-11 May 2001.

[17] PRODAS (Projectile Rocket Ordnance Design & Analysis System) V3, Technical Manual, Arrow Tech Associates, Inc.

[18] Zecevic B., Catovic A., Terzic J., Serdarevic - Kadic S., Analysis of influencing factors of mortar projectile reproduction process on fragment mass distribution, 13th Seminar "New trends in research of energetic materials", University of Pardubice, Pardubice, Chech Republic, April 21-23, 2010.

[19] Catovic A., Zecevic B., Terzic J., Analysis of terminal effectiveness for several types of HE projectiles and impact angles using coupled numerical-CAD technique, 12th Seminar "New trends in research of energetic materials", University of Pardubice, Pardubice, Chech Republic, April 1-3 2009.

[20] Zecevic B; Terzic J., Catovic A., Serdarevic-Kadic S., Influencing Parameters on HE Projectiles With Natural Fragmentation, 9th Seminar "New Trends in Research of Energetic Materials", University of Pardubice, Pardubice, Chech Republic, April 19-21, 2006.

[21] Static testing of high explosive munitions for obtaining fragment spatial distribution, US Army Combat Systems, APG, Maryland, 1993.

[22] Anon: Manufacture of Projectiles, Projectile Components, and Cartridge Cases for Artillery, Tank Main Armament, and Mortars, MIL-HDBK-756(AR), April 1991

[23] Valery Shikunova, New Life for Projectile Bodies, http://milparade.udm.ru/23/037.htm